Digital Radiography Versus Conventional Radiography in Chest Imaging: Diagnostic Performance of a Large-Area Silicon Flat-Panel Detector in a Clinical CT-Controlled Study

Marietta Garmer[1]
Svenja P. Hennigs[1]
Horst J. Jäger[1]
Felicitas Schrick[1]
Thomas van de Loo[1]
Andreas Jacobs[1]
Axel Hanusch[1]
Andreas Christmann[2]
Klaus Mathias[1]

OBJECTIVE. The objective of this study was to compare the diagnostic performance of a digital large-area silicon flat-panel detector with that of a conventional screen-film system in clinical chest imaging using abnormal findings documented by CT as the reference standard.

SUBJECTS AND METHODS. Eighty patients (46 men and 34 women; age range,18–91 years; mean age, 63 years) who underwent CT of the chest were examined with the new digital radiography system, which is based on a 43 × 43 cm silicon flat-panel detector, and with a conventional screen-film system, which is used routinely in clinical practice. Posteroanterior and lateral radiographs were obtained. Four radiologists analyzed the digital and conventional images separately for chest abnormalities and rated the images using a five-level scale of confidence; CT was used as the reference standard. Diagnostic value was assessed using receiver operating characteristic curves for each abnormality.

RESULTS. No significant differences were found between the area under the receiver operating characteristic curve of the digital and that of the conventional radiography method for almost all investigated criteria. The only exception was mediastinal abnormalities, for which the digital method provided better results than the conventional method ($p < 0.05$).

CONCLUSION. The diagnostic performance of the new large-area silicon flat-panel detector is equivalent or superior to that of the conventional screen-film system for clinical chest imaging and can replace conventional radiography systems. This new technology offers transmission and storage possibilities inherent to digital radiology that would facilitate daily practice and reduce the initial high costs in the long-term.

The role of digital radiology in radiology practice is a topic of continuing discussion as storage and transmission possibilities of digital information are increasing rapidly [1–4].

Image quality and diagnostic performance of these new techniques should be at least as good as those of conventional systems. On the other hand, disadvantages for patients, such as an increase of radiation dose, must be avoided. Furthermore, a new technique should be easy to perform in daily practice.

Chest radiographs are the most frequently obtained images in diagnostic radiology. Chest radiology is highly demanding because there are special technical requirements that result from the wide range of tissue densities [2, 5]. The main advantages of conventional screen-film systems are high spatial resolution, good uniformity over a large area, high sensitivity, easy handling, and low cost, but these systems are limited by the small exposure range of the film [4]. Using wide-latitude film and performing the technique at a high kilovoltage are suitable to overcome this problem to a certain extent.

Digital systems provide a wide dynamic range, which is preferable in chest imaging. The first step in digital chest radiology was the use of storage phosphor plates, which provide images of equivalent quality compared with those of conventional screen-film systems [4–6]. However, a higher radiation dose is needed to achieve a similar contrast resolution [7]. The second step was to use the selenium-drum detector, which was shown to produce images superior to those obtained using conventional screen-film systems [8–13] and the storage phosphor technique [14, 15], in the depiction of anatomic regions.

Recently, direct-readout radiography systems were developed. These systems are flat-panel X-ray detectors with either an integrated charge-coupled device or an integrated thin-

Received May 17, 1999; accepted after revision June 29, 1999.

Presented at the annual meeting of the American Roentgen Ray Society, New Orleans, May 1999.

[1]Department of Clinical Radiology, Staedtische Kliniken Dortmund, Beurhausstra. 40, 44137 Dortmund, Germany. Address correspondence to M. Garmer.

[2]Computing Center and Department of Statistics, University of Dortmund, August-Schmidt-Stra. 12, 44221 Dortmund, Germany.

AJR 2000;174:75–80

0361–803X/00/1741–75

film transistor (TFT) readout mechanism. Various types of TFT detectors have been studied [16–18]. All detectors are based on amorphous silicon TFT technologies, but each is combined with different types of converter arrays, which convert X-ray beams to electric charges directly or indirectly. Findings from a phantom study in chest imaging [19] and clinical studies in skeletal radiology [20, 21] have shown that this new electronically readable detector is promising.

In this study, the diagnostic performance of a digital large-area silicon flat-panel detector was compared with that of a conventional screen-film system in clinical chest imaging using abnormal findings documented by CT as the reference standard.

Subjects and Methods

Patients

From June to August 1998, 80 patients (46 men and 34 women; age range, 18–91 years; mean age, 63 years) from different clinical departments who underwent CT and radiography of the chest with a conventional screen-film system were examined. All patients had one or more radiographic abnormalities (range, 1–6). Posteroanterior and lateral chest radiographs were obtained with a digital system. All examinations were performed within 48 hr. Written consent was obtained from each patient and the study was approved by the institutional review board before digital radiographs were obtained.

Digital Radiography

A new flat-panel detector system (CXDI-11; Canon, Tokyo, Japan) was used to perform the digital chest radiography with the patient in an erect position. The detector uses a TFT and a metal insulator semiconductor-type photoelectric converter fabricated together on a glass substrate. Both components are made from hydrogenated amorphous silicon. The sensor has 2688 × 2688 pixels, with each pixel being 160 µm. The active area is 43 × 43 cm (17 × 17 inches). The system uses a rare-earth scintillator (terbium-doped gadolinium dioxide sulfide) coupled to the array. X-ray beams are converted to visible light at the scintillator, and the visible light is detected by the metal insulator semiconductor-type photoelectric converter. The resultant signals are scanned by the TFTs. This type of detector is characterized by a high signal-to-noise ratio and provides a spatial resolution of 3.1 line pairs per millimeter; dynamic range is approximately four digits. Signals are digitized in a 12-bit format producing a 4096 gray-scale image. Within 3 sec a preview image is displayed on an operation panel to allow the technician to check that body-positioning is correct and exposure is adequate. Image data can be postprocessed, printed, or archived as digital information.

We used a standard X-ray tube (SRO 33/100; Philips, Hamburg, Germany) and a standard high-voltage generator (HFG 650 R; Communications and Power Industries, Ontario, Canada); the automatic exposure control was adjusted to a 400-speed class system requested by the German guidelines for diagnostic radiology. The system included a moving grid (40 lines per centimeter; ratio = 12). Exposure specifications were 125 kVp and a 200-cm film-focus distance. These specifications are concordant with the German guidelines for diagnostic radiology.

No individual postprocessing of the images was performed. To produce an overall appearance that was comparable with that of conventional radiographs, all data were processed with one defined parameter set that was adjusted during the installation phase of the system. This processing included a gray-scale look-up table, dynamic range compression, and adaptive unsharp masking for edge enhancement. Images were transferred to a laser imager (Ektascan 190 laser printer; Kodak, Stuttgart, Germany) to be printed on laser films (35 × 43 cm) (Ektascan EHN7; Kodak).

Conventional Radiography

Conventional examinations were performed using an automatic chest film changer (Thoramat; Siemens, Erlangen, Germany) combined with a latitude ultraviolet screen-film system (Ultravision L; Sterling, Bad Homburg, Germany); posteroanterior and lateral radiographs were obtained with the patient in an erect position. The spatial resolution that can be achieved with this technique is 5.6 line pairs per millimeter. Exposure specifications were set to be similar to those used to obtain the digital radiographs (e.g., 400-speed class, 125 kVp, and 200-cm film-focus distance), leading to comparable radiation doses for both methods. However, the exact entrance exposure for patients was not measured. A moving grid (40 lines per centimeter; ratio = 12) was used.

CT

Helical CT of the chest was performed (Somatom Plus; Siemens) with an 8-mm collimation, a table speed of 10 mm/sec, and 8-mm reconstruction intervals. Exposure parameters were 137 kVp and 145 mA with a 1-sec scan time. Sixty milliliters of IV nonionic contrast material (iopromide [Ultravist 300]; Schering, Berlin, Germany) was administered by power injection at a rate of 2 ml/sec. Images were reconstructed using a soft-tissue algorithm and were displayed at mediastinal window settings (width, 240 H; level, 60 H) and at lung window settings (width, 2000 H; level, –500 H).

Image Evaluation

The diagnoses that served as the reference standard were established by consensus of three radiologists who did not participate in the receiver operating characteristic (ROC) curve analysis. The consensus diagnoses were based on a review of CT scans and knowledge of each patient's history. The presence of abnormal findings was rated according to seven collective criteria (i.e., categories of abnormalities) and four single criteria (i.e., abnormalities rated additionally because of their special importance with regard to diagnostic or therapeutic consequences). The panel then checked image quality and confirmed consistent findings on digital and conventional radiographs to exclude possible changes between the two exposures.

The images were assessed for abnormalities (collective criteria), which were divided into categories. The category of pleural abnormalities (n = 38 [47.5%]) consisted of pleural effusion, pneumothorax, and pleural thickening. Pulmonary abnormalities (n = 51 [63.8%]) were defined as alveolar infiltration, atelectasis, interstitial disease, pulmonary masses and nodules, cavitation, bullae, and focal fibrosis. Mediastinal abnormalities (n = 33 [41.3%]) were defined as mediastinal masses, cardiomegaly, aortic aneurysm, and diaphragmatic hernia. Chest wall abnormalities (n = 16 [20.0%]) included rib fractures and evidence of mastectomy. Scoliosis, disk degeneration, osteophytes, and vertebral deformity were classified as spinal abnormalities (n = 53 [66.3%]). Catheter material and clips were classified as foreign bodies (n = 25 [31.3%]). Calcifications (n = 38 [47.5%]) could be noted as pleural calcification, vascular calcification, or other calcification.

From these categories, single criteria were extracted and rated additionally because of their special importance with regard to diagnostic or therapeutic consequences. These single criteria were pulmonary nodules (n = 21 [26.3%]), mediastinal masses (n = 19 [23.8%]), interstitial disease (n = 11 [13.8%]), and pleural effusion (n = 14 [17.5%]). Pulmonary nodules were measured and divided into the following subgroups according to their size: smaller than 1 cm (n = 12 [57.1%]), 1–2 cm (n = 6 [28.6%]), and greater than 2 cm (n = 3 [14.3%]). In three patients with multiple nodules of different sizes the smallest nodule was considered, so the numbers represent number of cases and not the number of nodules.

For the ROC analysis, further image evaluation using the same list of criteria was performed independently by four different board-certified radiologists. The radiologists were asked to determine whether each collective and single criterion was visible using the following five-level rating scale of confidence: definitely not present, 1; probably not present, 2; equivocal, 3; probably present, 4; or definitely present, 5. In addition, the observers noted the location of the lesion on a diagram of the lung. There were 80 digital and 80 conventional image-pairs, each consisting of posteroanterior and lateral radiographs. Digital and conventional image-pairs were given to the observers in randomized order to avoid bias in interpretation. The observers had to evaluate the digital and conventional examinations separately. Examinations of the same patient were viewed with a time interval of at least 6 weeks to minimize learning effects. Observers were not aware of the patient's history. Image evaluation was always performed under equal conditions such as room light or viewing boxes; interpretation time was unlimited. Digital and conventional images were not identified as such but could easily be rec-

ognized because of the specific properties of conventional and laser radiographs.

Data Analysis

ROC analysis was used to compare the performance of digital versus conventional radiography using the nonparametric method developed by deLong et al. [22]. This method takes into account that the empiric results for both radiographic techniques performed on the same individuals are correlated. All two-sided confidence intervals for the area under the ROC curves and for the difference between both areas are given at the 95% level. For the calculation, 1760 values per observer were needed (11 criteria × 80 patients × two methods). The computations and the plot were generated with a statistical analysis software (SAS; SAS Institute, Cary, NC).

Results

Digital and Conventional Radiography Ratings Versus the Reference Standard

Table 1 summarizes the evaluation results of the digital and conventional radiography methods relative to the diagnoses established by CT images. Definite findings (a rating of 5, definitely present) occurred more often using conventional radiographs than digital radiographs for all collective criteria. Calcifications were rated as "definitely present" more often using digital (50.9%) and conventional radiographs (51.6%) than the reference standard (47.5%). For all other criteria, definite ratings using digital and conventional radiography were equal to or less frequent than the reference standard.

ROC Analysis of Digital versus Conventional Radiography

The area under the ROC curve depends on the different criteria and ranges from 0.687 (mediastinal abnormalities, conventional method) to 0.953 (foreign bodies, digital method) (Table 2). No significant differences were found between the area under the ROC curve of the digital and conventional methods for almost all criteria considered. The single exception was the collective criterion mediastinal abnormalities, for which the digital method gave better results than the conventional method ($p < 0.05$) (Table 2 and Fig. 1). However, in all criteria except two (chest wall abnormalities and calcifications), the digital system performed equally to or slightly better than the conventional system without being statistically significant (Table 2).

Interobserver Variability for the ROC Analysis

Table 2 shows the differences of the areas under the ROC curves for all the observers. These differences of the area under the ROC curve of the digital radiography minus the corresponding area of the conventional radiography range from 0.064 (mediastinal abnormalities) to –0.023 (calcifications). Regarding these differences for each observer these quantities differ by less than 0.1 from the quantity which is calculated for all observers. Overall, no large differences among the ratings of the four observers were found. However, the observed area under the ROC curve for mediastinal abnormalities for the digital method was greater than the corresponding area for the conventional method for observer 1 (difference = 0.079), observer 2 (difference = 0.103), and observer 3 (difference = 0.091), whereas the opposite was true for observer 4 (difference = –0.025).

Detection of Pulmonary Nodules Categorized by Size

In 21 patients, pulmonary nodules were definitely detected on CT. Categorized by size, the nodules there were smaller than 1 cm in 12 of the 21 patients. On digital images, these nodules were detected by the four observers in 39 observations (probably present, $n = 3$; definitely present, $n = 36$). In nine observations, the nodules were missed and rated as definitely not present. On conventional images, the nodules were detected in 34 observations (probably present, $n = 3$; definitely present, $n = 31$). The nodules were missed in 12 observations (definitely not present, $n = 9$; probably not present, $n = 3$). Two observations were equivocal. The second subgroup consisted of six patients with nodules of between 1 and 2 cm. On digital images, the nodules were detected by the four observers in 22 observations (probably present, $n = 1$; definitely present, $n = 21$). In two observations, the nodules were missed and rated as definitely not present. On conventional images, the nodules were detected in 20 observations (probably present, $n = 3$; definitely present, $n = 17$). The nodules were missed in four observations (definitely not present, $n = 3$; probably not present, $n = 1$). The third subgroup consisted of three patients with nodules of greater than 2 cm. The nodules were detected by the four observers on all 12 digital observations (probably present, $n = 1$; definitely present, $n = 11$) and in all 12 conventional observations (definitely present, $n = 12$). No ROC analysis for these subgroups was performed because the subsamples were small, only 12, six, and three, respectively. However, the data indicate that both radiographic methods performed similarly for these 21 patients.

TABLE 1 Digital and Conventional Radiography Ratings Versus Reference Standard (CT) for 80 Patients

Criteria	Reference Standard % positive	Ratings of Digital Radiographs (%)					Ratings of Conventional Radiographs (%)				
		1	2	3	4	5	1	2	3	4	5
Collective											
Pleural abnormalities	47.5	40.3	9.4	2.2	9.7	38.4	40.0	6.6	1.9	12.8	38.8
Pulmonary abnormalities	63.8	30.6	2.5	2.5	13.8	50.6	27.8	5.0	1.6	11.9	53.8
Mediastinal abnormalities	41.3	56.9	13.4	9.7	8.1	11.9	54.4	14.4	7.5	8.8	15.0
Chest wall abnormalities	20.0	65.0	22.5	1.9	3.4	7.2	64.7	19.4	2.2	2.2	11.6
Spinal abnormalities	66.3	22.2	5.6	0.9	10.6	60.6	20.9	3.8	1.6	11.9	61.9
Foreign bodies	31.3	70.0	0.3	0.0	0.0	29.7	69.7	0.0	0.3	0.0	30.0
Calcifications	47.5	37.2	4.7	1.6	5.6	50.9	33.1	7.5	0.3	7.5	51.6
Single											
Pulmonary nodules	26.3	62.5	6.6	1.3	4.1	25.6	61.6	9.4	2.5	3.8	22.8
Mediastinal masses	23.8	70.9	11.9	8.1	5.6	3.4	69.1	14.7	5.3	5.9	5.0
Interstitial disease	13.8	75.0	4.7	1.6	5.0	13.8	67.8	6.3	0.9	6.3	18.8
Pleural effusion	17.5	61.3	19.7	1.9	4.4	12.8	64.7	17.5	1.9	3.8	12.2

Note.—Four observers classified findings using the following five-level scoring system: 1, definitely not present; 2, probably not present; 3, equivocal; 4, probably present; and 5, definitely present.

TABLE 2 Receiver Operating Characteristic (ROC) Analysis of Digital Versus Conventional Radiography

Criteria	Digital Radiography		Conventional Radiography		Difference	
	Area	95% Confidence Interval[a]	Area	95% Confidence Interval[a]	Area	95% Confidence Interval[b]
Collective						
Pleural abnormalities	0.839	0.795–0.882	0.797	0.750–0.844	0.042	–0.007–0.091
Pulmonary abnormalities	0.903	0.867–0.938	0.877	0.836–0.918	0.026	–0.022–0.074
Mediastinal abnormalities	0.752	0.700–0.803	0.687	0.632–0.743	0.064[c]	0.012–0.117
Chest wall abnormalities	0.710	0.634–0.785	0.732	0.656–0.809	–0.022	–0.102–0.057
Spine abnormalities	0.697	0.640–0.754	0.697	0.640–0.754	0.000	–0.059–0.059
Foreign bodies	0.953	0.925–0.981	0.943	0.913–0.973	0.010	–0.027–0.046
Calcifications	0.708	0.656–0.760	0.731	0.680–0.782	–0.023	–0.070–0.024
Single						
Pulmonary nodules	0.893	0.849–0.937	0.879	0.832–0.925	0.014	–0.034–0.062
Mediastinal masses	0.733	0.668–0.799	0.693	0.626–0.759	0.041	–0.006–0.088
Interstitial disease	0.881	0.827–0.935	0.833	0.769–0.897	0.048	–0.023–0.120
Pleural effusion	0.852	0.784–0.919	0.830	0.760–0.899	0.022	–0.030–0.074

[a] 95% confidence interval of the area under the ROC curve.

[b] 95% confidence interval of the difference between the areas under the ROC curves (the value for digital radiography minus the value for conventional radiography).

[c] Difference between the areas under the ROC curves was significant at the 5% level ($p = 0.017$).

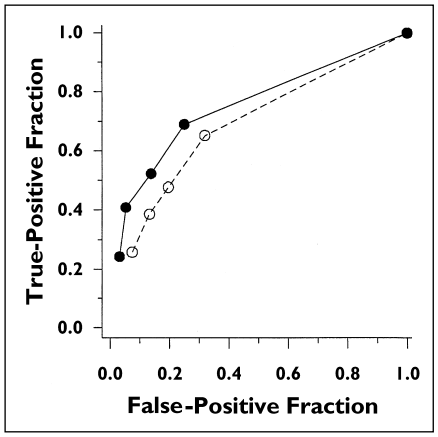

Fig. 1.—Mediastinal abnormalities revealed by digital (*solid line*) and conventional (*dashed line*) radiography. Area under receiver operating characteristic curve of digital radiography is greater than corresponding area of conventional radiography, indicating better performance of digital radiography for diagnosis of mediastinal abnormalities.

Discussion

Digital radiography continues to evolve rapidly as detector technology improves. Large-area direct-readout flat-panel X-ray detectors promise rapid access to the digital image for diagnosis. The flat-panel characteristic allows multipurpose use with bucky tables and rotating units. Ultimately, the flat-panel detector system based on TFT arrays will probably be the most promising technique in digital radiography. These systems achieve a detective quantum efficiency, which exceeds the performance of storage phosphor plates and conventional screen-film systems and is comparable with the performance of the selenium-drum detector [16, 18]. These systems can be divided into two classes: those with a mechanism that converts X-ray beams into electric charges directly and those with a mechanism that converts X-ray beams into electric charges indirectly. Both detectors are based on amorphous silicon TFT technologies currently used in liquid crystal for the electronic charge readout [18]. The direct-conversion system uses a continuous amorphous selenium layer that directly converts X-ray beams to electronic charges [17]. The indirect-conversion system requires a two-step process for X-ray detection: a scintillator converts the X-ray beams into visible light, and light is then converted into an electric charge by photodetectors, such as amorphous silicon photodiodes [16]. Nevertheless, the converter and the TFT cannot be formed in the same process at the same time. Progress in fabrication has allowed the creation of a large-area detector with a TFT and a metal insulator semiconductor-type photoelectric converter together on a glass substrate. This is simpler in construction, which leads to a lower rate of array defects, and can be fabricated at a low cost (Yamazaki T et al., presented at the annual meeting of the Radiological Society of North America, November 1997).

Which of these systems will become the preferred solution for the future remains unclear. However, image quality is substantially influenced by the type used. Physical indicators, such as the detective quantum efficiency, can describe the overall system performance, but there is no physical measurement that correlates perfectly with perceived diagnostic quality. MacMahon et al. [23] have already shown that a pixel size of 200 µm, leading to a lower spatial resolution than that of conventional screen-film systems, is sufficient for digital chest imaging. Finally, the ability of radiologists to detect lesions determines whether a new imaging technique is superior to existing systems. Therefore, observer studies with separate presentation of digital and conventional radiographs are the most conclusive methods [18]. ROC analysis clearly provides the best approach by which to measure image-based diagnostic performance studies [8, 13, 24].

To our knowledge, no other clinical study has dealt with the diagnostic performance of a flat-panel detector in chest radiography. A previous study performed in our department investigated the observer preference for the depiction of normal anatomic structures in a side-by-side view of conventional radiographs and digital flat-panel radiographs. The results showed an equal or higher score for most of the considered regions, but performance was worse for the hilum and aortopulmonary window in the lateral view (Hennigs SP et al., presented at the European Congress of Radiology, March 1999).

Strotzer et al. [19] investigated the observer preference of another indirect-conversion flat-panel detector with a scintillator based on cesium iodide. In this phantom study of cases of simulated chest lesions, comparison of digital images with images

from a screen-film system showed a statistically significant better result of the digital system for linear structures and micronodular lesions. Performance of pulmonary nodules and reticular patterns was the same. In skeletal radiology, the indirect-conversion detector [20] and the selenium-based direct-conversion detector [21] revealed an image quality equivalent or superior to that of screen-film radiographs at comparable doses.

In our study, more definite ratings for the conventional images occurred; this finding is probably associated with the fact that the observers were more accustomed to conventional images. Thus, the better performance of the digital images is more striking. The overestimation of calcifications in both digital and conventional images can be explained by projection effects of overlying structures.

One of the major advantages of the digital system is the wide dynamic range of the detector and the histogram equalization. These characteristics explain the improved contrast throughout the image and allow better visualization of low-contrast regions, such as the mediastinum. Clinical studies of diagnostic performance in digital radiology with CT serving as the gold standard for lesion detection only exist for the selenium-drum technique and the storage phosphor technique. No statistically significant difference was found for the diagnostic performance of the selenium-drum technique compared with that of a conventional chest system [8, 25]. Digital storage phosphor imaging was shown to be superior to conventional film radiography for CT-documented mediastinal lesions and pulmonary opacities of greater than 2 cm in diameter. For all other types of pulmonary lesions and pleural abnormalities, both systems were equivalent [26, 27].

In our study, no significant differences were found for the detection of CT-documented abnormalities in digital flat-panel radiography compared with that of conventional screen-film radiography for almost all criteria considered. We only found a significantly better result for the imaging of mediastinal abnormalities in digital radiography. However, the collective criterion mediastinal abnormalities contained mediastinal masses, cardiomegaly, aortic aneurysm, and diaphragmatic hernia. Referring to the more important single criterion, mediastinal masses, the difference in diagnostic performance was not statistically significant. Furthermore, observer 4 showed a smaller area under the ROC curve for the digital method than for the conventional method; however, overall we found no severe differences in diagnostic ability among the observers. Empirically for all criteria except two (chest wall abnormalities and calcifications), the digital system performed equally to or better than the conventional system.

Noting the distribution of the sizes of pulmonary nodules, in an attempt to describe different case difficulties, showed that digital and conventional imaging allowed similar diagnostic performance even for small pulmonary nodules. Thus, the lower spatial resolution had no impact on the diagnostic performance in our patients. This finding is consistent with the findings in the studies investigating the selenium-drum technique and the storage phosphor technique [8, 19, 25, 26].

In addition to various observer-preference studies with side-by-side comparison of radiographs in digital radiography, this CT-controlled study of diagnostic performance serves as a complement in imaging technique evaluation. Our results show an equal or better rate of detection of CT-documented abnormalities on digital radiographs relative to conventional radiographs. This study was designed as a comparison between a silicon flat-panel system and a conventional screen-film system; digital radiographs were intentionally obtained with an image appearance comparable with that of screen-film radiographs without a systematic study of the postprocessing. Other investigators have suggested that appropriate postprocessing could improve diagnostic performance because moderate edge enhancement at high spatial frequency would compensate for reduced spatial resolution that is limited by the pixel size of the detector [28, 29]. Nevertheless, individual postprocessing is time-consuming and not acceptable in daily practice. On the other hand, direct readout is timesaving; this advantage should be taken into account in systematic cost analysis, which is important when considering the introduction of new techniques. Immediately checking the patient's body position and the overall image quality reduces wait time and increases the patient's comfort. Integration of a new technique in picture archiving and communication systems will be an inevitable precondition [1]. Dose reduction is another promising advantage of this new flat-panel technology, which has also been shown for skeletal radiology and simulated chest lesions [19, 20]. Further investigations should prove this for clinical chest radiography.

We conclude that the diagnostic performance of the new large-area silicon flat-panel detector is equivalent or superior to that of the conventional screen-film system in clinical chest imaging and can replace conventional radiographic systems. This new technology offers the transmission and storage possibilities inherent to digital radiology, which could facilitate daily practice and reduce the initial high costs in the long-term.

Acknowledgments

We thank Mark Pattison for reviewing this manuscript and E. A. Hühn and the technicians in our department for their help.

References

1. Tylen U. Digital chest radiography: clinical aspects. *J Digit Imaging* **1995**;8[suppl]:15–19
2. MacMahon H, Vyborny C. Technical advances in chest radiography. *AJR* **1994**;163:1049–1059
3. Glazer HS, Muka E, Sagel SS, Jost RG. New techniques in chest radiography. *Radiol Clin North Am* **1994**;32:711–729
4. Busch HP, Lehmann KJ, Drescher P, Georgi M. New chest imaging techniques: a comparison of five analogue and digital methods. *Eur Radiol* **1992**;2:335–341
5. Slone RM, van Metter R, Senol E, Muka E, Pilgram TK. Effect of exposure variation on the clinical utility of chest radiographs. *Radiology* **1996**;199:497–504
6. Ishigaki T, Endo T, Ikeda M, et al. Subtle pulmonary disease: detection with computed radiography versus conventional chest radiography. *Radiology* **1996**;201:51–60
7. Tylén U. Stimulable phosphor plates in chest radiology. *Eur Radiol* **1997**;73[suppl]:S83–S86
8. van Heesewijk HP, van der Graaf Y, de Valois JC, Vos JA, Feldberg MA. Chest imaging with a selenium detector versus conventional film radiography: a CT-controlled study. *Radiology* **1996**;200:687–690
9. van Heesewijk HP, Neitzel U, van der Graaf Y, de Valois JC, Feldberg MA. Digital chest imaging with a selenium detector: comparison with conventional radiography for visualization of specific anatomic regions of the chest. *AJR* **1995**;165:535–540
10. Neitzel U, Maack I, Gunther-Kohfahl S. Image quality of a digital chest radiography system based on a selenium detector. *Med Phys* **1994**;21:509–516
11. Floyd CE Jr, Baker JA, Chotas HG, Delong DM, Ravin CE. Selenium-based digital radiography of the chest: radiologists' preference compared with film-screen radiographs. *AJR* **1995**;165:1353–1358
12. Zaehringer M, Krug B, Dolken W, Gossmann A, Lackner K. Can digital selenium detector-based chest imaging replace standard analogue film screen imaging? *Rofo Fortschr Geb Rontgenstrahlen Neuen Bildgeb Verfahr Erganzungsbd* **1997**;167:4–10
13. Kotter E, Einert A, Merz C, et al. Comparison between a screen-film system and a selenium radiography system. An ROC study using simulated thoracic lesions. *Invest Radiol* **1999**;34:296–302
14. Schaefer-Prokop CM, Prokop M, Schmidt A, Neitzel U, Galanski M. Selenium radiography

versus storage phosphor and conventional radiography in the detection of simulated chest lesions. *Radiology* **1996**;201:45–50
15. Beute GH, Flynn MJ, Eyler WR, Samei E, Spizarny DL, Zylak CJ. Chest radiographic image quality: comparison of asymmetric screen-film, digital storage phosphor, and digital selenium drum systems—preliminary study. *RadioGraphics* **1998**;18:745–754
16. Siewerdsen JH, Antonuk LE, El-Mohri Y, Yorkston J, Huang W, Cunningham IA. Signal, noise power spectrum, and detective quantum efficiency of indirect-detection flat-panel imagers for diagnostic radiology. *Med Phys* **1998**;25:614–628
17. Rowlands JA, Zhao W, Blevis IM, Waechter DF, Huang Z. Flat-panel digital radiology with amorphous selenium and active-matrix readout. *RadioGraphics* **1997**;17:753–760
18. Chotas HG, Dobbins JT, Ravin CE. Principles of digital radiography with large-area, electronically readable detectors: a review of the basics. *Radiology* **1999**;210:595–599
19. Strotzer M, Gmeinwieser J, Voelk M, Fruend R, Seitz J, Feuerbach S. Detection of simulated chest lesions with normal and reduced radiation dose: comparison of conventional screen-film radiography and a flat-panel X-ray detector based on amorphous silicon. *Invest Radiol* **1998**;33:98–103
20. Strotzer M, Gmeinwieser J, Volk M, et al. Clinical application of a flat-panel X-ray detector based on amorphous silicon technology: image quality and potential for radiation dose reduction in skeletal radiography. *AJR* **1998**;171:23–27
21. Piraino DW, Davros WJ, Lieber M, et al. Selenium-based digital radiography versus conventional film-screen radiography of the hands and feet: a subjective comparison. *AJR* **1999**;172:177–184
22. deLong ER, deLong DM, Clarke-Pearson DL. Comparing the areas under two or more correlated receiver operating characteristic curves: a nonparametric approach. *Biometrics* **1988**;44:837–845
23. MacMahon H, Vyborny CJ, Metz CE, et al. Digital radiography of subtle pulmonary abnormalities: a ROC study of effect of pixel size on observer performance. *Radiology* **1986**;158:21–26
24. Metz CE. Some practical issues of experimental design and data analysis in radiological ROC studies. *Invest Radiol* **1989**;24:234–245
25. Woodard PK, Slone RM, Sagel SS. Detection of CT-proved pulmonary nodules: comparison of selenium-based digital and conventional screen-film chest radiographs. *Radiology* **1998**;209:705–709
26. Schaefer CM, Greene R, Oestmann JW, et al. Digital storage phosphor imaging versus conventional film radiography in CT-documented chest disease. *Radiology* **1990**;174:207–210
27. Buckley KM, Schaefer CM, Greene R, et al. Detection of bullous lung disease: conventional radiography vs digital storage phosphor radiography. *AJR* **1991**;156:467–470
28. Correa J, Souto M, Tahoces PG, et al. Digital chest radiography: comparison of unprocessed and processed images in the detection of solitary pulmonary nodules. *Radiology* **1995**;195:253–258
29. Nodine CF, Liu H, Miller WT Jr, Kundel HL. Observer performance in the localization of tubes and catheters on digital chest images: the role of expertise and image enhancement. *Acad Radiol* **1996**;3:834–841